Determination of the Onset of Shear Thinning of Polydimethylsiloxane

Dimiter Hadjistamov

DECE GmbH, Helvetierstr.15, 4125 Riehen, Switzerland

Received 25 September 2006; accepted 6 November 2007
DOI 10.1002/app.27685
Published online 12 February 2008 in Wiley InterScience (www.interscience.wiley.com).

ABSTRACT: The shear stress and the first normal stress difference were simultaneously measured in shear flow start-up experiments and a subsequent stress relaxation. The measured polydimethylsiloxane show shear thinning flow behavior with a first Newtonian region up to the shear rate at the onset of shear thinning. We found that the shear stress and the first normal stress difference have an equal shear rate at the onset of shear thinning. The shear stress at the onset of shear thinning does not depend on the molecular weight of the polymer and on temperature. Similar to the viscosity master curve, it is possible to create a normal stress master curve, outgoing from the first normal stress coefficient. The shear rate at the onset of shear thinning is estimated from the viscosity master curve and the shear rate at the onset of normal stress thinning from the normal stress master curve. The shear stress and the first normal stress difference have similar transient behavior with start-up stress curves without maximum in stress growth experiments with shear rates from the first Newtonian region. The shear flow start-up experiment with the shear rate at the onset of shear thinning leads to the first indication of an overshoot of the start-up curve. The shear flow start-up experiments with shear rates from the shear thinning region show start-up curves with a maximum for the shear stress and for the first normal stress difference. It was found that the shear rate at the onset of shear thinning and the shear rate at the onset of normal stress thinning, determined by the shear flow start-up measurements, are equal to the values obtained from the master curves. © 2008 Wiley Periodicals, Inc. J Appl Polym Sci 108: 2356–2364, 2008

Key words: shear rate at the onset of shear thinning; shear stress at the onset of shear thinning; normal stress master curve; transient behavior

INTRODUCTION

Polydimethylsiloxane (PDMS) with the monomer unit [SiO $(CH_3)_2$] are inert and nontoxic. PDMS are widely used as caulks, sealants and in a lot of greases, adhesives, and lubricants. PDMS are utilized as defoaming agent also in the food industry as E900. PDMS are used for breast implants, as a calibration fluid,[1] and as matrix fluid for model suspensions in the rheology.[2–11] Several authors studied the rheological behavior of polydimethylsiloxane.[12–18] Rheological measurements as well as ultrasonic tests are used for the characterization of PDMS.[19–22] It is noteworthy that Verdier et al.[21] and Longin et al.[22] obtained via this method the whole dynamic shear master curve with over 10 decades.

The PDMS show, like polymer melts, polymer solutions, and some suspensions, shear thinning flow behavior. The main characteristic of the systems with shear thinning behavior is the existence of a first Newtonian region with a zero-shear viscosity η_0 (Fig. 1). The molecular entanglements appear proportional to the shear deformation and the shear stress remains proportional to the shear rate in this region.

The point where the first Newtonian region ends and, respectively, the shear thinning region begins is the onset of shear thinning with the shear rate at the onset of shear thinning $\dot{\gamma}_c$ (Fig. 1) and with the shear stress at the onset of shear thinning τ_c. The determination of the shear rate and the shear stress at the onset of shear thinning is not so easy. The shear rate at the onset of shear thinning can be approximately evaluated ($\dot{\gamma}_c'$) from the cross over point of the elongated first Newtonian region and the tangent to the shear thinning section.[23] We use the crossover point of the elongated first Newtonian region and the straight line of the first 2–5 points of the shear thinning region, which leads to a more accurate determination of the shear rate at the onset of shear thinning. The shear stress at the onset of shear thinning can be calculated with the ''rodi'', empirical model of viscosity master curve.[24] We do not find values for the onset of shear thinning of PDMS in the literature.

The time-related flow behavior is widely used for the characterization of the rheological behavior, for example, of polyethylene melts;[25] suspensions;[26–30]

Correspondence to: D. Hadjistamov (dhadjistamov@datacomm.ch).

Journal of Applied Polymer Science, Vol. 108, 2356–2364 (2008)

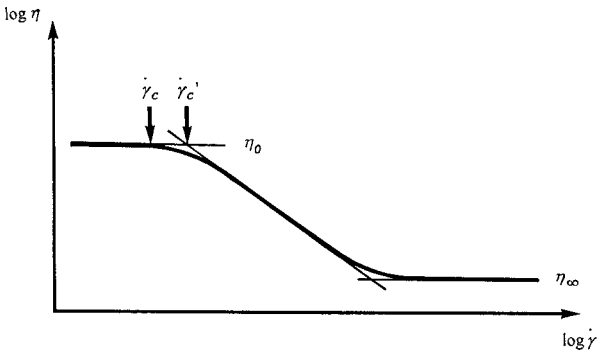

Figure 1 Schematical viscosity curve of systems with shear thinning flow behavior.

lyotropic hydroxypropylcellulose solutions;[31] thixotropy;[32,33] rheopexy;[34] and polydimethylsiloxane.[15,35]

The aim of this contribution is to determine the onset of shear thinning of PDMS outgoing from steady state and transient measurements of the shear stress and the first normal stress difference.

EXPERIMENTAL

The following polydimethylsiloxane were investigated: M20′000, M50′000, M80′000, M100′000, and M500′000 from BAYER AG. The weight average molecular weights are 68, 85, 97, 104, and 164 kg/mol (BAYER AG). The relation between the weight and the number average molecular weight is $\sim$ 2.3. The rheological measurements were carried out with a Weissenberg-Rheogoniometer (WRG), model R18 with cone-plate (6° with diameter 5 cm) and plate–plate with a diameter of 5 cm at 25 $\pm$ 0.2°C.

The Rheogoniometer was modified according to Meissner,[36] for the measurement of the first normal stress difference.

The shear flow start-up of the shear stress τ (with cone-plate and plate–plate) and the first normal stress difference N_1 (cone-plate) were simultaneously measured as a function of the time with a constant shear rate $\dot{\gamma} = \text{const}$ (Fig. 2).

This is a kind of determination of the transient or time-related behavior of the systems. The shear stress

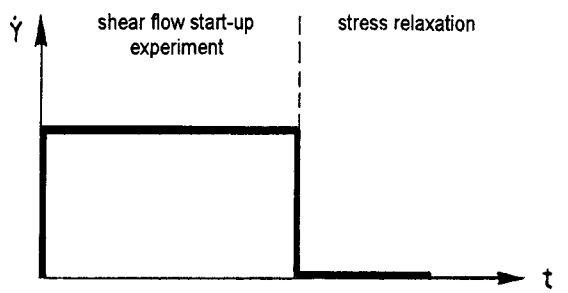

Figure 2 Shear flow startup experiment and stress relaxation.

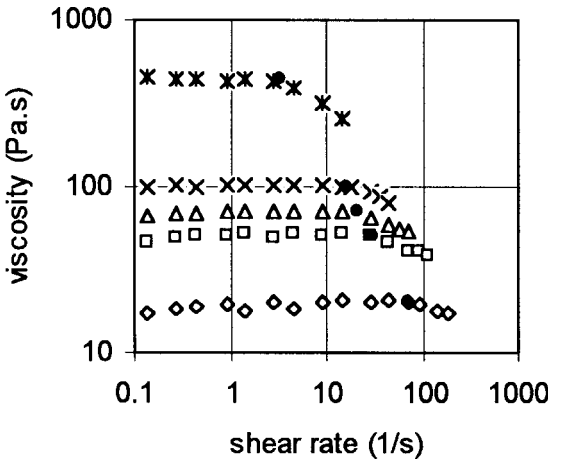

Figure 3 Viscosity curves of silicone oils—◇ M20′000, □ M50′000, Δ M80′000, × M100′000, ∗ M500′000, and ● onset of shear thinning (WRG, plate–plate, 25 $\pm$ 0.2°C).

and the first normal stress difference were recorded with the time t. The start-up experiments were carried out up to the steady state shear stress τ_s and the steady state normal force N_{1s} were reached. The points of the flow curves and normal stress curves represent the steady state values from the shear flow start-up experiments.

Just after the steady state values are reached, it is possible to stop the shear flow. The relaxation of the shear stress and normal force begins after the cessation of the shear flow ($\dot{\gamma} = 0$). The shear stress and the first normal stress difference were also simultaneously recorded during the stress relaxation until the steady state values were reached.

RESULTS AND DISCUSSION

Steady shear rheological properties

Figure 3 shows the viscosity curves of different polydimethylsiloxane (PDMS). The viscosity curves, obtained by a cone-plate and plate–plate devices are equal, but the plate–plate system is more precise at higher shear rates.

The zero-shear viscosity can be estimated from Figure 3 (Table I). The dependence of the zero-shear viscosity on the molecular weight will be discussed later (Fig. 10).

The shear rate and the shear stress at the onset of shear thinning can be determined from the crossover of the Newtonian region and the straight line from the first 2–5 measured points of the shear thinning region (Fig. 3 and Table 1).

The values of the shear stress at the onset of shear thinning are τ_c = 1500 $\pm$ 100 Pa. The shear stress at the onset of shear thinning appears for the measured PMDS at different shear rates.

TABLE I
Values for the Onset of Shear Thinning

	Shear rate at the onset of shear thinning $\dot{\gamma}_c$ (1/s)	Shear stress at the onset of shear thinning $\tau_c = \eta_0.\dot{\gamma}_c$ (Pa)	Zero-shear viscosity, η_0 (Pa s)
M 20′000	70	1400	20
M 50′000	30	1500	50
M 80′000	21	1470	70
M 100′000	16	1600	100
M 500′000	3.3	1450	440

One can calculate from the viscosity master curve (Fig. 4)

$$\frac{\eta}{\eta_0} = f(\eta_0 \cdot \dot{\gamma}) \quad (1)$$

the average value for shear stress at the onset of shear thinning (τ_{cm}) for all measured PDMS as τ_{cm} = 1500 Pa. The shear rate at the onset of shear thinning will be 15 1/s for the silicone oil M100′000.

Figure 5 represents the dependence of the zero-shear viscosity on the shear rate at the onset of shear thinning.

The silicone oils with higher zero-shear viscosity (corresponds to higher molecular weights) seem to be more sensitive to shear deformation. These systems have smaller values for the shear rate at the onset of shear thinning, i.e., the shear thinning region begins earlier.

The points of Figure 5 are satisfactorily correlated by the equation

$$\eta_0 = A.\ \dot{\gamma}_c^n \quad (2)$$

The value of the straight line slope is $n = -1$. Consequently, the constant A represents the shear stress at the onset of shear thinning for all silicone oils $A = \tau_{cm}$. This value can be obtained from the linear regression as A = τ_{cm} = 1524 Pa. If we consider also the points for the silicone oil M500′000 at 25, 40, 60 and 80°C,[37] the value will be A = τ_{cm} = 1467 Pa. This means that the shear stress at the onset of shear thinning τ_{cm} is independent of the polymer molecular weight and temperature and can be assumed to be a material constant for the measured silicone oils. The shear stress at the onset of shear thinning seems to depend only on the polymer type—for example 1500 Pa for PDMS, 267 Pa for LDPE,[24] and 3209 Pa for the Polyisobutylene Oppanol B15.[24] This relation can be represented by the dependence of the shear stress at the onset of shear thinning on the molecular weight of the monomers Mw_M (Fig. 6).

The experimental points can be satisfactorily correlated to the straight line with a slope of n = 0.52:

$$\tau_c = A.\,\mathrm{Mw}_M^n \quad (3)$$

We assume that there is a correlation between the shear stress at the onset of shear thinning and the molecular weight of the monomers, but further measurements are necessary to confirm this correlation.

First normal stress difference

The dependence of the first normal stress difference N_1 on the shear rate leads to straight lines with a slope of n = 2 up to the shear rate at the onset of normal stress thinning (Fig. 7).

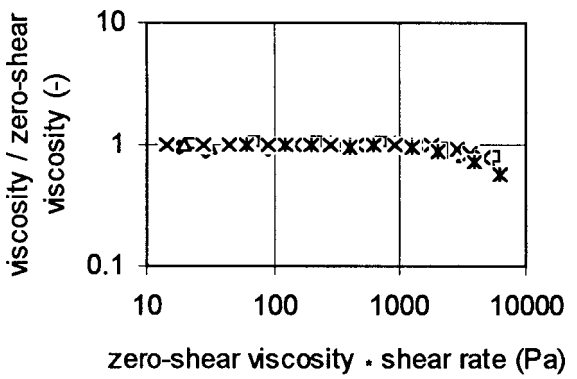

Figure 4 Viscosity master curve of the silicone oils—◇ M20′000, □ M50′000, Δ M80′000, × M100′000, and ∗ M500′000 (WRG, plate–plate, 25 ± 0.2°C).

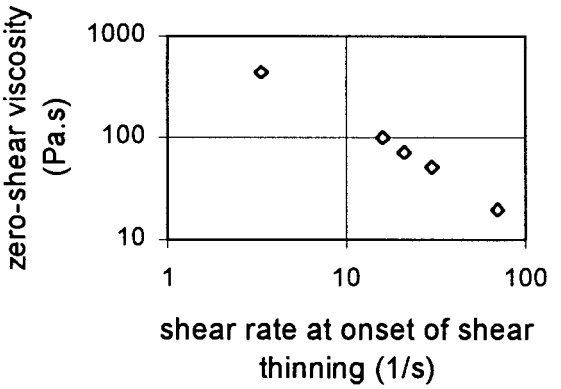

Figure 5 Dependence of the zero-shear viscosity on the shear rate at the onset of shear thinning for the measured silicone oils (Table I).

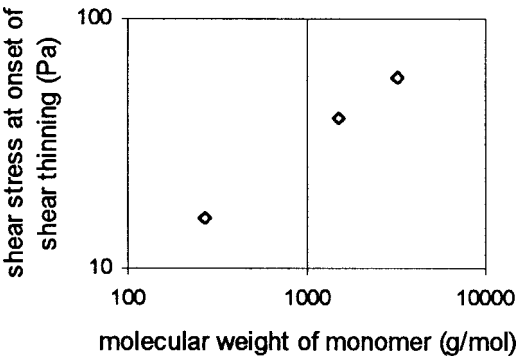

Figure 6 Dependence of the shear stress at the onset of shear thinning on the molecular weight of the monomers of LDPE, PDMS and Polyisobutylene Oppanol B15.

It is well known that there is a quadratic dependence of the first normal stress difference on the shear rate. As a result of that, it is possible to calculate the well known first normal stress coefficient Ψ_1:

$$\Psi_1 = N_1/\dot{\gamma}^2 \tag{4}$$

Figure 8 represents the dependence of the first normal stress coefficient on the shear rate.

All systems have a region of the first normal stress coefficient with points that do not change with the shear rate. Similar to the zero-shear viscosity, these points will be called zero-first normal stress coefficient Ψ_{10} (Fig. 8). The point where the zero-first normal stress coefficient region ends will be called the onset of normal stress thinning. It is possible to estimate the values for the zero-first normal stress coefficient and the onset of normal stress thinning from Figure 8 (Table II).

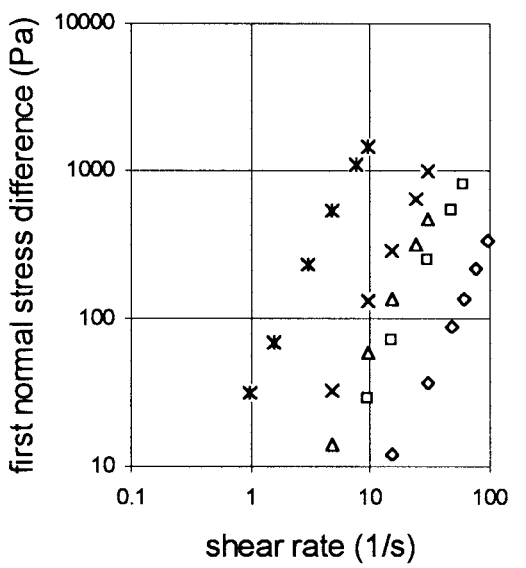

Figure 7 Normal stress curves of the silicone oils—◇ M20′000, □ M50′000, Δ M80′000, × M100′000, and ∗ M500′000 (WRG, cone-plate, 25 ± 0.2°C).

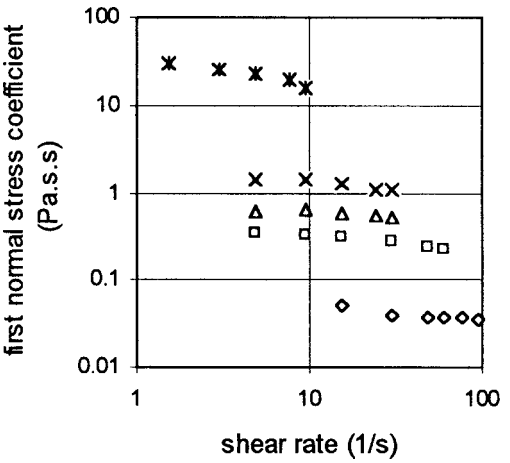

Figure 8 First-normal stress coefficient curves of the silicone oils—◇ M20′000, □ M50′000, Δ M80′000, × M100′000, and ∗ M500′000 (WRG, cone-plate, 25 ± 0.2°C).

Similar to the shear stress at the onset of shear thinning, it is to be expected that the normal stress at the onset of normal stress thinning have nearly equal values. These values differ indeed from 112 to 315 Pa, due to the fact that the data for the normal force are hard to analyze and the determination of this point is not so exact. Further measurements are necessary to confirm this point.

The shear rates at the onset of normal stress thinning (Table 2) have comparable values with the shear rates at the onset of shear thinning (Table 1).

We can now create, similar to the viscosity master curve, the first normal stress master curve (Fig. 9):

$$\Psi_1/\Psi_{10} = f(\Psi_{10}.\dot{\gamma}^2) \tag{5}$$

It is possible to determine the first normal stress difference at the onset of normal stress thinning for all systems as N_{1Cm} = 260 Pa from the normal stress master curve (Fig. 9). This value is independent of the molecular weight of the silicone oils and is about 5.8 times smaller, compared to the shear stress at the onset of shear thinning from the viscosity master (Fig. 4) curve with 1500 Pa. One can calculate from Eq. (5) the shear rate at the onset of normal stress thinning for the silicone oil M100′000 as $\dot{\gamma}_{cN1}$ = 13.6 1/s. We can maintain that the shear rate at the onset of shear thinning for M100′000 (15 1/s from the viscosity master curve) and the shear rate at the onset of normal stress thinning occur nearly at the same shear rate.

The dependence of the zero-shear viscosity and the zero-first normal stress coefficient on the weight average molecular weight is plotted on Figure 10.

The zero-shear viscosity increases with the higher molecular weights of the silicone oils (Fig. 10). We

TABLE II
Onset of Normal Stress Thinning for the First Normal Stress Coefficient

	Shear rate at the onset of normal stress thinning, $\dot{\gamma}_c$ (1/s)	Normal stress at the onset of normal stress thinning, N_{1C} (Pa)	Zero-first normal stress coefficient, Ψ_{10} (Pa s^2)
M 20′000	75	214	0.038
M 50′000	19	112	0.31
M 80′000	20	244	0.61
M 100′000	15	315	1.40
M 500′000	3	261	29

found,[38] for the dependence of zero-shear viscosity on weight average molecular weight (Mw) at 25°C the well-known relation:

$$\eta_0 = 3.4 \times 10^{-16} \cdot \mathrm{Mw}^{3.48} \quad (6)$$

Kataoka and Ueda,[13] found for Mw ≥ 55000 at 25°C the relation:

$$\eta_0 = 2.35 \times 10^{-16} \cdot \mathrm{Mw}^{3.53} \quad (7)$$

El Kissi et al.,[15] introduced this relation after Mills,[14] in the WLF relation and obtained for 23°C

$$\eta_0 = 4.73 \times 10^{-18} \cdot \mathrm{Mw}^{3.70} \quad (8)$$

There is really a good agreement between eqs. (6) and (7).

The dependence of the zero-first normal stress coefficient on the weight average molecular weight leads also to a straight line (Fig. 10)

$$\Psi_{10} = \mathrm{B.\ Mw}^{7.43} \quad (9)$$

It is interesting to note that the power of 7.43 is roughly twice the power of eq. (6). This hangs together with the fact that the normal stress is proportional to the shear rate to power two in the zero-first normal stress coefficient region and on the contrary, the shear stress is directly proportional to the shear rate in the zero-shear viscosity region.

The ratio between zero-shear viscosity and zero-first normal stress coefficient is 526 for the silicone oil M20′000. The ratio decreases with the molecular weight, for M500′000 is only 15. The higher molecular weights lead to a stronger interaction between the molecules and to a better physical structure, especially of the elastic behavior. The extrapolation of these two functions from Figure 10 leads to the point of intersection at a weight average molecular weight of ~ 220 kg/mol.

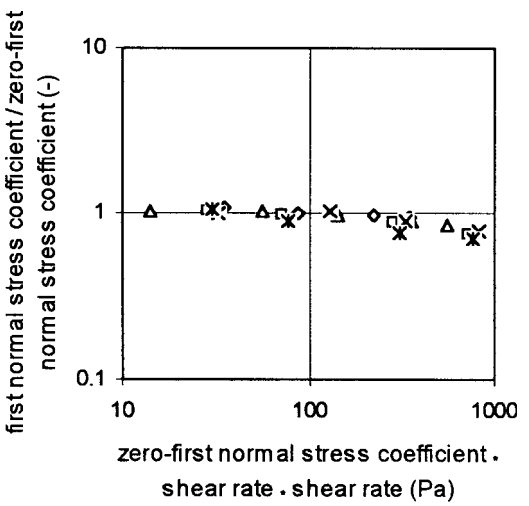

Figure 9 Normal stress master curve of the silicone oils—◇ M20′000, □ M50′000, Δ M80′000, × M100′000, and ∗ M500′000 (WRG, cone-plate, 25 ± 0.2°C).

Transient behavior

It is well known[39] that start-up curves without maximum occur at stress growth experiments with low shear rates from the viscoelastic region. The start-up

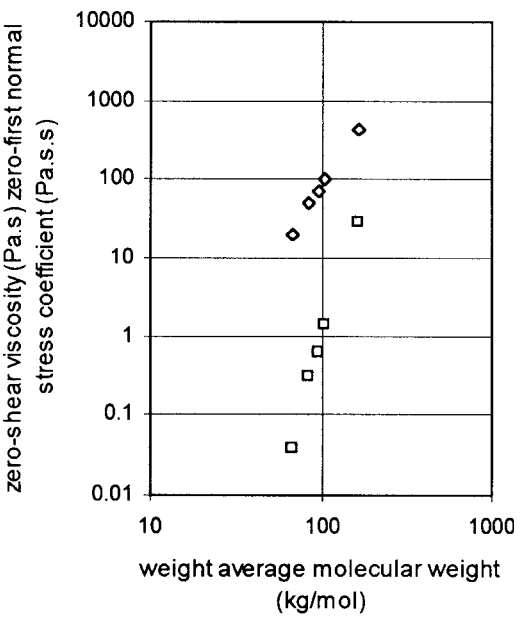

Figure 10 Dependence of zero-shear viscosity and zero-first normal stress coefficient on the weight average molecular weight. ◇ zero-shear viscosity (Table 1), □ zero-first normal stress coefficient (Table II) (WRG, 25 ± 0.2°C).

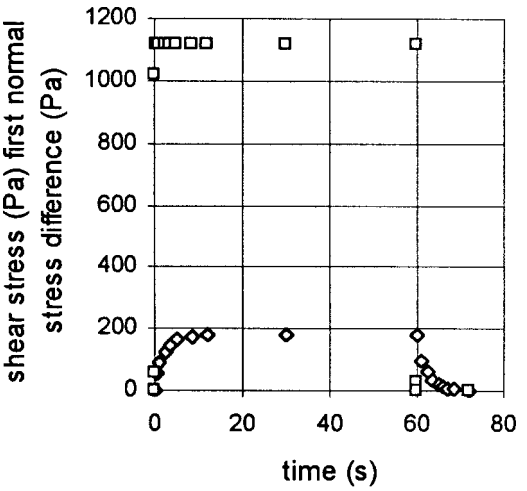

Figure 11 Shear flow start-up experiment with 11.25 1/s and stress relaxation of the silicone oil M100′000 (□ shear stress, ◇ first normal stress difference, WRG, cone-plate 6°).

curves with larger shear rates,[39] (from the shear thinning region) run through a maximum before approaching the steady state value. But there is no advice when the form of the start-up curve changes. We assume that the the shear rate at onset of shear thinning is important according to the form of the start-up curve.

The shear rate at the onset of shear thinning for the silicone oil M100′000 was determined as $\dot{\gamma}_c$ = 15 1/s and the shear rate at onset of normal stress thinning as $\dot{\gamma}_{cN1}$ = 13.6 1/s. Accordingly, time related behavior of the silicone oil M100′000 were investigated in shear flow start-up experiments with shear rates from the first Newtonian region (11.25 1/s), near the onset of shear thinning (14.2 1/s) and after the onset of shear thinning (17.8 1/s and 22.14 1/s), i.e., from the shear thinning region.

Figure 11 shows the shear flow start-up experiment with the shear rate of 11.25 1/s, i.e., from the first Newtonian region.

The shear stress and the first normal stress difference show, as expected,[39] start-up curves without maximum. Shear flow start-up experiments, carried out with smaller shear rates exhibit also start-up curves without a maximum. The steady state value of the shear stress is reached about ten times faster compared to the steady state value of the first normal stress difference. In the first Newtonian region, the shear stress is proportional to the shear rate and there is a quadratic dependence of the first normal stress difference on the shear rate. The zero-shear viscosity and the zero-normal stress coefficient do not change with the shear rate in this region. The polymer molecules can rearrange themselves in this region, despite higher shear deformation, up to a very special shear rate, the shear rate at onset of shear thinning. We assume that the onset of shear thinning is an important value for a system.

The shear stress and normal stress decline towards the zero point on relaxation, i.e., no residual shear stress τ_R and residual normal stress N_R are observed.

A shear flow start-up experiment was carried out with the shear rate of 14.2 1/s, i.e., near to the shear rate at the onset of shear thinning ($\dot{\gamma} \approx \dot{\gamma}_c$) (Fig. 12).

This stress growth experiment leads to a start-up curve with a small overshoot for the shear stress, with a maximum τ_m = 1397 Pa and a steady state value τ_s = 1391 Pa. The start-up curve for the first normal stress difference also exhibits a maximum with N_{1m} = 267 Pa and a steady state value of N_{1S} = 265 Pa. We assume that the first appearance of a maximum is a sign of the onset of shear thinning. Correspondingly, we can decide that this shear rate is the shear rate at the onset of shear thinning $\dot{\gamma}_c$ = 14.2 1/s and the shear rate at the onset of normal stress thinning $\dot{\gamma}_{cN1}$ = 14.2 1/s. This value is close to the values $\dot{\gamma}_c$ = 15 1/s and $\dot{\gamma}_{cN1}$ = 13.6 1/s, determined from the viscosity and normal stress master curves (Figs. 4 and 9).

The shear rate at onset of shear thinning can overcome the hydrodynamic state of the first Newtonian region. A breakdown of the physical structure occurs at the onset of shear thinning. This is visible also on the flow and normal stress coefficient curves, where the shear stress and first normal stress coefficient begin to decline from the constant values of the zero-shear viscosity and the zero-normal stress coefficient.

Figures 13 and 14 represent shear flow startup experiments with shear rates, higher than the shear rate at the onset of shear thinning ($\dot{\gamma} > \dot{\gamma}_c$), i.e., from the shear thinning region.

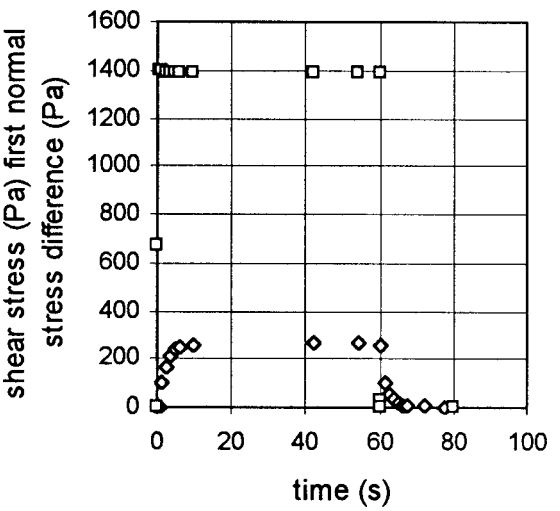

Figure 12 Shear flow start-up experiment with 14.2 1/s and stress relaxation of the silicone oil M100′000 (□ shear stress, ◇ first normal stress difference, WRG, cone-plate 6°).

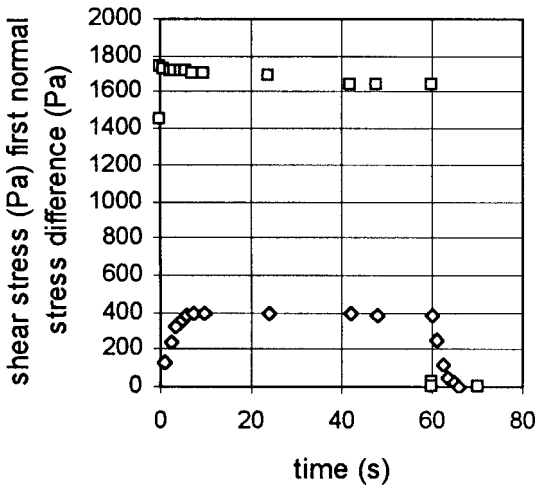

Figure 13 Stress growth experiment with 17.8 1/s and stress relaxation of the silicone oil M100′000 (□ shear stress, ◇ first normal stress difference, WRG, cone-plate 6°).

The start-up curves show an overshoot (Figs.13 and 14). The shear stress declines from a maximum of 1731 Pa to the steady state value of 1644 Pa (Fig. 13). The difference between maximum value and steady state values is bigger for the stress growth experiment with 22.5 1/s (Fig. 14) compared to the experiment with 17.8 1/s (Fig. 13). The maximum increases, as expected,[39] with increasing shear rate of the stress growth experiments (compare Figs. 12–14). The same is observed for the start-up curves of the first normal stress difference (compare Figs. 12–14). The start-up curves of the first normal stress difference are similar, but the steady state values will be obtained later. Shear flow experiments with the shear rate at the onset of shear thinning and higher shear rates $\dot{\gamma} \geq \dot{\gamma}_c$ lead to start-up curves with maximum for the shear stress and the normal stress.

Some authors,[32,40] try to explain the start-up curve with overshoot. The first part with increasing shear stress is observed in accordance with the elastic deformation of the system. The decrease of shear stress after the maximum corresponds to the destruction of the system. The increase of the shear rate from the shear thinning region causes an increase of the destruction of the system's physical structure. This leads to an increasing difference between the maximum and the steady state values in the stress growth experiments.

The shear stress and the first normal stress difference decline towards the zero point on relaxation, no residual shear stress and no residual first normal stress difference are observed after the cessation of the steady shear flow (Figs. 11–14). No remaining structure exists after the stressing experiment that can opposes against the elastic returned springing of the strip bar to the starting point.

CONCLUSION

The measured PDMS show shear thinning flow behavior with a first Newtonian region and a shear thinning section. The point where the first Newtonian region ends and, respectively, the shear thinning region begins is the onset of shear thinning with the shear rate at the onset of shear thinning $\dot{\gamma}_c$ and with the shear stress at the onset of shear thinning τ_c. We think that the onset of shear thinning is an important point. One can say that the shear deformation or the shear rate affects at this point the beginning of the distortion of the hydrodynamic steady state of the systems. The shear stress at the onset of shear thinning is equal for all PDMS. This value can be estimated from the viscosity master curve or calculated from the dependence of the zero-shear viscosity on the shear rate at the onset of shear thinning.

From the quadratic dependence of the first normal stress difference on the shear rate, one can determine the first normal stress coefficient Ψ_1. The dependence of the first normal stress coefficient on the shear rate shows a region where the Ψ_1 does not change with the shear rate. This region will be called, similar to the zero-shear viscosity, zero-first normal stress coefficient Ψ_{10}. The point where the zero-first normal stress coefficient region ends will be called the onset of normal stress thinning. One can consequently assume that the zero-first normal stress coefficient region corresponds to the first Newtonian region. Similar to the shear stress at the onset of shear thinning, it is to be expected that the normal stress at the onset of normal stress thinning has nearly equal values. The values for the normal stress at onset of normal stress thinning are about 5.8 times smaller compared to the shear stress at the onset of shear thinning. Outgoing from the first normal stress

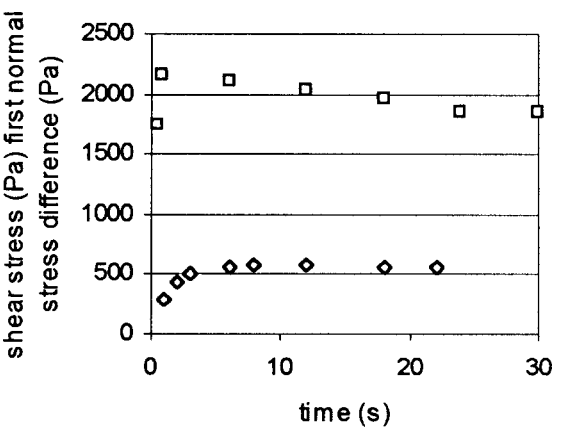

Figure 14 Stress growth experiment with 22.5 1/s and stress relaxation of the silicone oil M100′000 (□ shear stress, ◇ first normal stress difference, WRG, cone-plate 6°).

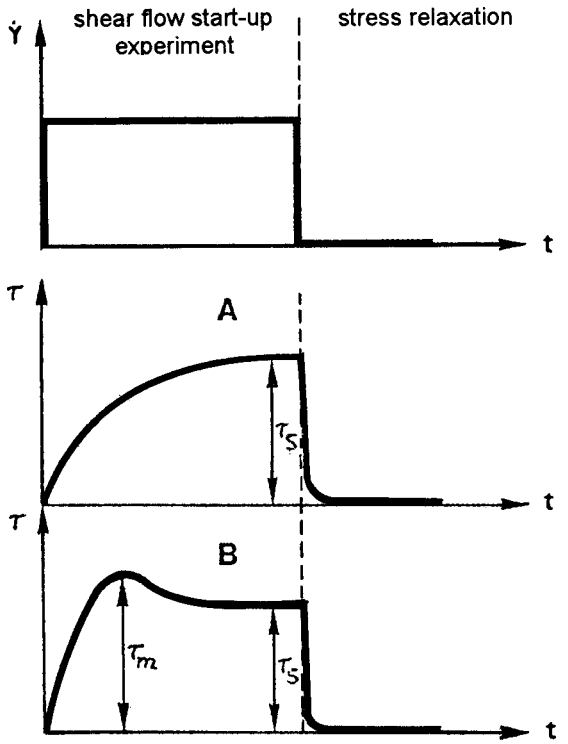

Figure 15 Time related flow behavior of shear thinning systems.

coefficient and the zero-first normal stress coefficient, it is possible to create the first normal stress master curve.

The shear rate at the onset of shear thinning for the measured PDMS is estimated from the viscosity master curve. The shear rate at the onset of normal stress is determined from the normal stress master curve. It was found that the values for the shear rate at the onset of shear thinning and the shear rate at the onset of normal stress thinning are equal.

The time-related flow behavior of the system with shear thinning flow behavior PDMS depends obviously on the shear rate of the shear flow start-up experiment. Shear stress and normal stress start-up curves without a maximum are obtained in stress growth experiments with shear rates below the shear rate at the onset of shear thinning ($\dot{\gamma} < \dot{\gamma}_c$) [Fig. 15(A)].

Shear flow experiments with the shear rate at the onset of shear thinning and higher shear rates $\dot{\gamma} \geq \dot{\gamma}_c$ lead to start-up curves with maximum for the shear stress and the normal stress [Fig. 15(B)]. We assume that the first overshoot of the start-up curve appears in the stress growth experiment with the shear rate at the onset of shear thinning. This is visible on the first overshoot in the shear flow start-up experiment. Accordingly, we can determine the shear rate at the onset of shear thinning and the shear rate at the onset of normal stress thinning from stress growth experiments. The shear rate at the onset of shear thinning and the shear rate at the onset of normal stress thinning, determined by the shear flow start-up measurements, are equal to the values, obtained from the viscosity and normal stress master curves. The effect of the shear rate of the stress growth experiment is the same for the shear stress and for the first normal stress difference.

The shear stress and the first normal stress difference decline towards the zero point on relaxation, no residual shear stress and no residual first normal stress difference are observed after the cessation of the steady shear flow. No remaining structure exists after the stressing experiment that can oppose against the elastic returned springing of the strip bar to the starting point.

References

1. Zeqiri, B. Ultrasonics 1989, 27, 314.
2. Cantu, T. S.; Caruthers, J. M. J Appl Polym Sci 1982, 27, 3079.
3. Ziegelbaur, R. S.; Caruthers, J. M. J Non-Newtonian Fluid Mech 1985, 17, 45.
4. Kosinski, L. E.; Caruthers, J. M. Rheol Acta 1986, 25, 153.
5. DeGroot, J. V., Jr.; Macosko, C. W.; Kume, T.; Hashimoto, T. J Colloid Interface Sci 1994, 166, 404.
6. Piau, J.-M.; Dorget, M.; Palierne, J.-F.; Pouchelon, A. J Rheol 1999, 43, 305.
7. Mall-Gleissle, S. E.; Gleissle, W.; McKinley, G. H.; Buggish, H. Rheol Acta 2002, 41, 61.
8. Hadjistamov, D. Appl Rheol 1993, 3, 113.
9. Hadjistamov, D. Appl Rheol 1995, 5, 29.
10. Hadjistamov, D. Appl Rheol 2002, 12, 297.
11. Hochstein, B. Dissertation: Rheologie von Kugel- und Fasesuspensionen mit viscoelastischen Matrixflüssigkeiten, 1997.
12. Barlow, A. J.; Harrison, G.; Lamb, J. Proc R Soc Lond Ser A 1964, 282, 228.
13. Kataoka, T.; Ueda, S. J Polym Sci A-1: Polym Chem 1967, 5, 3071.
14. Mills, N. J. Eur Polym J 1968, 5, 675.
15. El Kissi, N.; Piau, J. M.; Attané, P.; Turrel, G. Rheol Acta 1993, 32, 293.
16. Hadjistamov, D. Appl Rheol 1996, 6, 203.
17. Hadjistamov, D. Rheol Acta 1996, 35, 364.
18. Takahashi, T.; Kaschta, J.; Münstedt, H. Rheol Acta 2001, 40, 490.
19. Rahalkar, R. R.; Lamb, J.; Barlow, A. J.; Hawthorne, W.; Semlyen, J. A.; North, A. M.; Pethrick, R. A. Faraday Symp Chem Soc 1983, 18, 103.
20. Rahalkar, R. R.; Lamb, J.; Harrison, G.; Barlow, A. J.; Hawthorne, W.; Semlyen, J. A.; North, A. M.; Pethrick, R. A. Proc R Soc Lond Ser A 1984, 394, 207.
21. Verdier, C.; Longin, P.-Y.; Piau, M. Rheol Acta 1998, 37, 234.
22. Longin, P. Y.; Verdier, C.; Piau, M. J Non-Newtonian Fluid Mech 1998, 76, 213.
23. Schurz, J. J Polym Sci Part C: Polym Lett 1990, 28, 141.
24. Fisch, R. D.; Hadjistamov, D. GIT Labor-Fachzeitschrift 1998, 42, 1017.
25. Ranganathan, M.; Mackley, M. R.; Spitteler, P. H. J. J Rheol 1999, 43, 443.
26. Hadjistamov, D. Rheol Acta 1980, 19, 345.
27. Narumi, T.; See, H.; Honma, Y.; Hasegawa, T.; Takahashi, T.; Phan-Thien, N. J Rheol 2002, 46, 295.
28. Kolli, V. G.; Pollauf, E. J.; Gadala-Maria, F. J Rheol 2002, 46, 321.
29. Mohraz, A.; Solomon, M. J. J Rheol 2005, 49, 657.
30. Bekkour, K.; Leyama, M.; Benchabane, A.; Scrivener, O. J. J Rheol 2005, 49, 1329.

31. Hartmann, V.; Vermant, J.; Heinrich, E.; Mewis, J.; Moldenaers, P. J Rheol 2000, 44, 1417.
32. Barnes, H. A. J Non-Newtonian Fluid Mech 1997, 70, 1.
33. Dullaert, K.; Mewis, J. J Rheol 2005, 49, 1213.
34. Massalova, I.; Taylor, M.; Kharatiyan, E.; Malkin, A. Y. J Rheol 2005, 49, 839.
35. Gleissle, W.; Ohl, N. Rheol Acta 1990, 29, 261.
36. Meissner, J. J Appl Polym Sci 1972, 16, 2877.
37. Hadjistamov, D. Les Cahiers de Rheologie 1996, 15, 29.
38. Hadjistamov, D. In Proceedings of XIth Congress on Rheology; Moldenaers, P., Kreunings, R., Eds.; 1992; p 17.
39. Bird, B. R.; Armstrong, R. C.; Hassager, O. Dynamics of Polymeric Liquids; Vol. 1, Fluid Mechanics, 2nd ed., Wiley: New York, 1987.
40. Bekkour, K.; Leyama M.; Benchabane, A.; Scrivener, O. J Rheol 2005, 49, 1329.